



Red de Revistas Científicas de América Latina, el Caribe, España y Portugal
Sistema de Información Científica

Ricardo Carelli, Carlos Soria, Oscar Nasisi, Eduardo Freire
Stable AGV Corridor Navigation with Fused Vision-Based Control Signals
Dyna, vol. 70, núm. 140, noviembre, 2003, pp. 61-69,
Universidad Nacional de Colombia
Colombia

Available in: <http://www.redalyc.org/articulo.oa?id=49614006>



Dyna,
ISSN (Printed Version): 0012-7353
dyna@unalmed.edu.co
Universidad Nacional de Colombia
Colombia

[How to cite](#)

[Complete issue](#)

[More information about this article](#)

[Journal's homepage](#)

www.redalyc.org

Non-Profit Academic Project, developed under the Open Access Initiative

STABLE AGV CORRIDOR NAVIGATION WITH FUSED VISION-BASED CONTROL SIGNALS

RICARDO CARELLI

*Instituto de Automática, Universidad Nacional de San Juan
Av. San Martín Oeste, 5400 San Juan, Argentina.*

CARLOS SORIA

*Instituto de Automática, Universidad Nacional de San Juan
Av. San Martín Oeste, 5400 San Juan, Argentina.*

OSCAR NASISI

*Instituto de Automática, Universidad Nacional de San Juan
Av. San Martín Oeste, 5400 San Juan, Argentina.*

EDUARDO FREIRE

*Departamento de Física da Universidade Federal de Sergipe
Av. Marechal Rondon, s/n, Jardim Rosa Elze, São Cristovão/SE, Brazil.*

Colaboración especial para la Revista Dyna Nro. 140.

ABSTRACT: This work presents a control strategy for mobile robots navigating in corridors, using the fusion of the control signals from vision based controllers. To this aim two controllers are proposed to generate the control signals to be fused: one is based on the optical flow calculation and the other is based on the perspective lines in the corridor. Both controllers generate angular velocity commands to keep the robot navigating along the corridor, and compensate for the dynamics of the robot. The fusion of both control signals is made by using a Kalman filter. Stability of the resulting control system is analyzed. Experiments on a laboratory robot are presented to show the feasibility and performance of the proposed controller.

1 INTRODUCTION

Mobile robots are mechanical devices which are capable of operating in an environment with a certain degree of autonomy. The environment can be classified as structured when it is perfectly known and motion can be planned in advance, or as partially structured when there are uncertainties that imply some on-line planning of motions. Autonomous navigation is related to the capability of capturing environment information through external sensors, such as vision, distance or proximity sensors. Although distance sensors (e.g., ultrasound and laser types), which allow to detect obstacles and measure distance to walls

near the robot, are the most usual sensors, at present the tendency is towards vision sensors which supply better and a larger amount of information from images.

When autonomous mobile robots navigate within indoor environments (e.g., in public buildings or industrial facilities) they should be endowed the capability to move along corridors, to turn at corners and to come into rooms. As regards motion along corridors, some control algorithms have been proposed based on artificial vision. In [9], image processing is used to detect perspective lines and to guide the robot following the corridor centerline. This work assumes an elementary

control law and does not prove control stability. In [16], ceiling perspective lines are employed for robot guidance, but it also lacks a demonstration on system stability. Other authors have proposed to use the technique of optical flow for corridor centerline guidance. Some approaches incorporate two video cameras on the robot sides, and the optical flow is computed to compare the apparent velocity of image patterns from both cameras [14]. In [5], a camera is used to guide a robot along a corridor centerline or to follow a wall. In [15] perspective lines are used to find the absolute orientation within a corridor.

In general, these works do not present a stability analysis for the control system. On the other hand, the performance of the control system depends on environment conditions such as illumination, surface textures, perturbations from image quality loss, and other factors, all of which making that each individual controller not reach acceptable robust properties. A solution for this problem is to consider multiple controllers, based on different sensing information, which operate simultaneously. Although having the same control objectives, the controllers can be coordinated using the concept of behavior coordination [11]. Within this concept, the command fusion schemes accept a set of behavior instances that share the control of the whole system at all times.

Command fusion schemes can be classified into four categories: voting (e.g. DAMN [12], superposition (e.g. AuRA [1], Multiple Objective (e.g. Multiple Decision-Making Control [11]) and fuzzy logic (e.g. Multivaluated Logic Approach [13]). Another example of a command fusion strategy is the dynamic approach to behaviour-based robotics [3]. In this paper we consider the command fusion structure previously proposed in [8].

In the present work, two vision-based control algorithms for corridor navigation are presented. The first one uses the optical flow measured from the corridor's lateral walls to generate an angular velocity command for the mobile robot. The second scheme finds the perspective lines of the walls meeting the floor to generate the angular velocity command for the robot. The linear speed of the robot may either be kept constant or be

controlled, in order to achieve a smooth and cautious navigation. Both controllers are redundant, because they have the same control objective. They are based, however, in different principles, which turn difficult their fusion at sensorial level. Here, we propose a fusion of both commands to attain a control signal that allows a robust navigation along corridors. For the fusion, the control architecture via control output fusion is used, as proposed in [8], employing a Kalman filter that minimizes the uncertainty level in both controllers. This uncertainty is evaluated in terms of the sensing error and the environment conditions by means of a covariance function for each controller. A stability analysis of the resulting control system is done as well. The work also presents experimental results on a Pioneer 2 DX laboratory robot navigating at the Institute of Automatics, National University of San Juan, Argentina.

2 ROBOT AND CAMERA MODELS

A. Robot Model

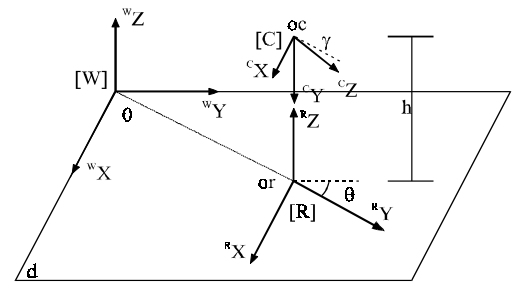


Figure 1. Coordinate systems.

Figure 1 represents the coordinate systems associated to the robot and the environment: a world system [W], a system [R] fixed to the robot and a system [C] fixed to the vision camera. Regarding Figure 1, the kinematic model of a unicycle type robot can be expressed as [7],

$$\begin{cases} \omega = \dot{\theta} \\ \dot{y} = v \cos(\theta) \\ \dot{x} = v \sin(\theta) \end{cases} \quad (1)$$

where ω is the angular velocity and v the linear velocity of the robot, $x \equiv {}^W x_{or}$, $y \equiv {}^W y_{or}$.

In order to compensate for vehicle dynamics, the dynamics model of the robot was obtained experimentally by step command response analysis. Of particular interest is the model relating $\omega_R \rightarrow \omega_y$, where ω_R is the reference angular velocity generated by the controller and sent to the robot, and ω_y is the measured angular velocity of the robot. The identified model is approximately represented by a second order linear model,

$$\omega_y = \frac{k_\omega a_\omega}{s^2 + b_\omega s + a_\omega} \omega_R \quad (2)$$

with $k_\omega = 0.45$, $a_\omega = 104.6$, $b_\omega = 9.21$.

B. Camera Model.

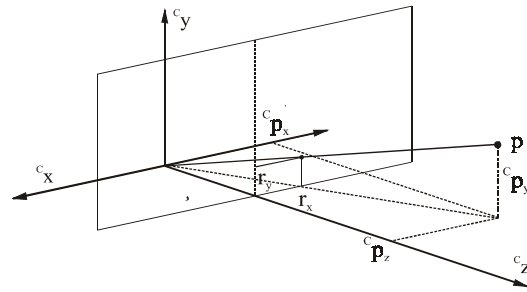


Fig. 2. Perspective projection camera model.

A pinhole model for the camera is considered. The following relationship can be immediately obtained from Figure 2,

$$r = \alpha \lambda \frac{p}{c p_z} \quad (3)$$

where r is the projection of a point p on the image plane, λ is the focal length of the camera and α is a scale factor.

C. Differential Camera-Robot Model

This subsection presents the kinematic relationship of the camera mounted on the

moving robot evolving with linear velocity v and angular velocity ω . The Coriolis equation renders the motion of a point P in a coordinate system with translational and rotational motion V and Ω ,

$$\dot{P} = -V - \Omega \times P \quad (4)$$

By time-deriving (3) and using both (4) and (3), the components of \dot{r} on the image plane are found as,

$$\dot{r}_x = \frac{-\lambda V_x + r_x V_z}{P_z} + \frac{\omega_x}{\lambda} r_x r_y - \omega_y \left(\lambda + \frac{r_x^2}{\lambda} \right) - \omega_z r_y \quad (5)$$

$$\dot{r}_y = \frac{-\lambda V_y + r_y V_z}{P_z} + \omega_x \left(\lambda + \frac{r_y^2}{\lambda} \right) - \frac{\omega_y}{\lambda} r_x r_y - \omega_z r_x \quad (6)$$

For the camera mounted on the robot's center and pointing forward, $V_x = V_y = 0$ and $\omega_x = \omega_z = 0$. Besides, by calling $v = V_z$, $\omega = \omega_y$, (5) and (6) can be written as,

$$\dot{r}_x = \frac{r_x v}{c p_z} - \omega \left(\lambda + \frac{r_x^2}{\lambda} \right) \quad \dot{r}_y = \frac{r_y v}{c p_z} - \frac{\omega}{\lambda} (r_x r_y) \quad (7)$$

which represent the differential kinematic equations for the camera mounted on the robot.

D. Model for the perspective lines.

For the design of one of the controllers, it is necessary to obtain the relation between the position and orientation of the robot and the projection of the perspective lines in the corridor on the image plane. The parallel lines resulting from the intersection of corridor walls and floor, are projected onto the image plane as two lines intersecting in the so-called vanishing point.

A point p in the global frame [W] can be expressed in the camera frame [C] as,

$${}^C p = {}^C R_W ({}^W p - {}^W p_{oc}) - {}^C R_R {}^R p_{oc}$$

where

$${}^C R_R = \begin{bmatrix} 1 & 0 & 0 \\ 0 & -\sin(\gamma) & -\cos(\gamma) \\ 0 & \cos(\gamma) & -\sin(\gamma) \end{bmatrix},$$

and

$${}^C R_W = \begin{bmatrix} \cos(\theta) & -\sin(\theta) & 0 \\ -\sin(\theta)\sin(\gamma) & -\cos(\theta)\sin(\gamma) & -\cos(\gamma) \\ \sin(\theta)\cos(\gamma) & \cos(\theta)\cos(\gamma) & -\sin(\gamma) \end{bmatrix}$$

with γ the camera tilt angle and θ the robot heading.

Considering the component-wise expressions for the pinhole camera model (3),

$$r_x = \alpha_x \lambda \frac{{}^C p_x}{{}^C p_z}, \quad r_y = \alpha_y \lambda \frac{{}^C p_y}{{}^C p_z} \quad (8)$$

any point in the global coordinate system is represented in the image plane as a projection point with coordinates

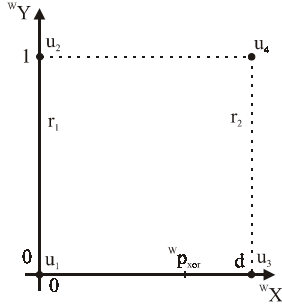


Figure 3. Guide lines in the corridor.

$$r_x = \alpha_x \lambda \frac{\cos(\theta)({}^W p_x - {}^W p_{xor}) - \sin(\theta)\cos(\gamma)({}^W p_x - {}^W p_{xor}) + \sin(\theta)({}^W p_y - {}^W p_{yor})}{\cos(\theta)\sin(\gamma)({}^W p_y - {}^W p_{yor}) - \sin(\gamma)h} \quad (9)$$

$$r_y = \alpha_y \lambda \frac{-\sin(\theta)\sin(\gamma)({}^W p_x - {}^W p_{xor}) - \sin(\theta)\cos(\gamma)({}^W p_x - {}^W p_{xor}) - \cos(\theta)\sin(\gamma)({}^W p_y - {}^W p_{yor}) - \cos(\gamma)h}{\cos(\theta)\sin(\gamma)({}^W p_y - {}^W p_{yor}) - \sin(\gamma)h} \quad (10)$$

Now consider the points $u_1 = [0 \ 0 \ 0]^T$, $u_2 = [0 \ 1 \ 0]^T$, $u_3 = [d \ 0 \ 0]^T$, $u_4 = [d \ 1 \ 0]^T$ that define the intersection lines $r_1 = (u_1, u_2)$ and $r_2 = (u_3, u_4)$ between corridor walls and floor, as illustrated in Figure 3. Based on (9) and (10), the following relationships are obtained for the slope of the perspective lines, the vanishing point

coordinates and the intersection of both lines with the horizontal axis in the image plane, Figure 4.

$$m_1 = \frac{\alpha_y}{\alpha_x} \frac{h \cos(\theta)}{(\cos(\gamma))^W p_{xor} + \sin(\theta)\sin(\gamma)h} \quad (11)$$

$$m_2 = \frac{\alpha_y}{\alpha_x} \frac{h \cos(\theta)}{(\cos(\gamma))^W p_{xor} - d + \sin(\theta)\sin(\gamma)h} \quad (12)$$

$$x_v = -\frac{\alpha_x \lambda \tan(\theta)}{\cos(\gamma)} \quad (13)$$

$$y_v = \alpha_y \lambda \tan(\gamma) \quad (14)$$

$$\frac{b_1}{m_1} = \frac{\alpha_x \lambda (\sin(\theta)\cos(\gamma)h - {}^W p_{xor}\sin(\gamma))}{h \cos(\theta)} \quad (15)$$

$$\frac{b_2}{m_2} = \alpha_x \lambda \frac{(d - {}^W p_{xor})\sin(\gamma) + h\sin(\theta)\cos(\gamma)}{h \cos(\theta)} \quad (16)$$

3 VISION BASED CONTROLLERS

A. Controller Based on the Optical Flow

The control proposal for navigation along the corridor is based on the calculation of optical flow [2] in two symmetric lateral regions on the image plane $r_{x1} = -r_{x2}$, Figure 5. From (7), the horizontal optical flow in these points is given by

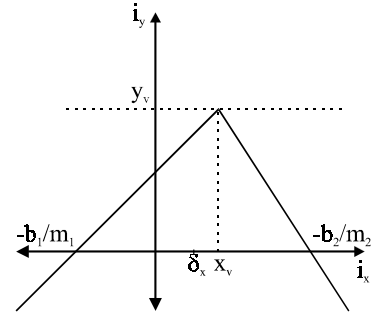


Figure 4. Perspective lines.

$$\dot{r}_{x1} = \frac{r_{x1}v}{P_{z1}} - \omega(\lambda + \frac{r_{x1}^2}{\lambda}) \quad (17)$$

$$\dot{r}_{x2} = -\frac{r_{x1}v}{P_{z1}} - \omega(\lambda + \frac{r_{x1}^2}{\lambda})$$

To navigate along the corridor centerline, the control objective on the image plane is to equate

the lateral optical flows $\dot{r}_{x1} = -\dot{r}_{x2}$. Then, from (17)

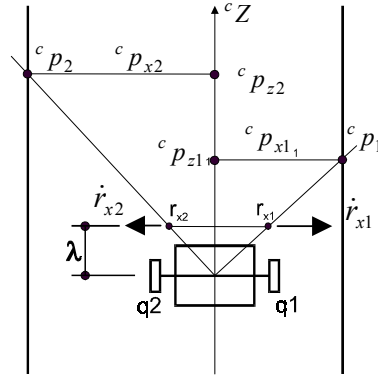


Figure 5. Schematics of the control proposal.

$$r_{x1}v\left(\frac{1}{c p_{z1}} - \frac{1}{c p_{z2}}\right) = 2\omega\left(\lambda + \frac{r_{x1}^2}{\lambda}\right) \quad (18)$$

In addition, if robot rotation $\omega = 0$, then $c p_{z1} = c p_{z2}$, which means that the robot is navigating along the corridor centerline. From (17), the vision model for the lateral optical flow measured at $r_{x1} = -r_{x2}$ is

$$\begin{pmatrix} \dot{r}_{x1} \\ \dot{r}_{x2} \end{pmatrix} = \begin{pmatrix} \frac{r_{x1}}{c p_{z1}} & -\left(\lambda + \frac{r_{x1}^2}{\lambda}\right) \\ \frac{r_{x2}}{c p_{z2}} & -\left(\lambda + \frac{r_{x1}^2}{\lambda}\right) \end{pmatrix} \begin{pmatrix} v \\ \omega \end{pmatrix} = J \begin{pmatrix} v \\ \omega \end{pmatrix} \quad (19)$$

where J is called the Jacobian of the robot-camera system.

Now, by considering the dynamic model of the robot (2),

$$\ddot{\omega} + b_{\omega}\dot{\omega} + a_{\omega}\omega = k_{\omega}a_{\omega}\omega_R \quad (20)$$

an inverse dynamics control law is regarded

$$\omega_R = \frac{1}{k_{\omega}a_{\omega}} \{\eta + b_{\omega}\dot{\omega}_y + a_{\omega}\omega_y\} \quad (21)$$

where η is a variable defined as,

$$\eta = \ddot{\omega}_d + k_{p\omega}(\omega_d - \omega) + k_{d\omega}(\dot{\omega}_d - \dot{\omega}) \quad (22)$$

In (22), ω_d is interpreted as the desired angular velocity, which is set to zero in order to comply with the control objective of maintaining a stable navigation along the corridor. Besides, $k_{p\omega}, k_{d\omega}$ are design gains. In order to include the exteroceptive information of optical flow, the inverse of relation (19),

$$\begin{bmatrix} v \\ \omega \end{bmatrix} = J^{-1}\dot{r}, \quad J^{-1} = \{j_{i,j}^{-1}\} \quad (23)$$

$$\omega = j_{21}^{-1}\dot{r}_1 + j_{22}^{-1}\dot{r}_2$$

is substituted in the term of angular velocity error in (22),

$$\omega_R = \frac{1}{k_{\omega}a_{\omega}} [-k_{p\omega}(j_{21}^{-1}\dot{r}_1 + j_{22}^{-1}\dot{r}_2) - k_{d\omega}\dot{\omega}_y + b_{\omega}\dot{\omega}_y + a_{\omega}\omega_y] \quad (24)$$

By combining (21) and (20) the closed-loop equation is obtained as,

$$\ddot{\omega} + k_{d\omega}\dot{\omega} + k_{p\omega}\omega = 0$$

which implies $\omega(t) \rightarrow 0$ as $t \rightarrow \infty$. From (17) with $\omega = 0$, $\dot{r}_{x1} = -\dot{r}_{x2}$. Then, the unique navigation condition is verified at the centerline of the corridor.

B. Controller Based on Perspective Lines

It is important to express the control objective of navigating along the corridor centerline in terms of the image features from perspective lines. The control objective is achieved when the slope of both perspective lines become equal, that is when x_v -the vanishing point- and δ_x -the middle point between the intersection of both perspective lines with the horizontal axis- are equal to zero, Figure 4. In the workspace, orientation robot error θ and position robot error relative to the center of the corridor $\tilde{x} = {}^w p_{xor} - d/2$ are defined. These errors can be expressed in terms of the image features x_v and δ_x . Equation (13) can be written as,

$$x_v = K_1 \tan(\theta), \quad K_1 = -\frac{\alpha_x \lambda}{\cos(\gamma)}$$

from which,

$$\theta = \arctan\left(\frac{x_v}{K_1}\right) \quad (25)$$

Besides,

$$\delta_x = -\frac{1}{2}\left(\frac{b_1}{m_1} + \frac{b_2}{m_2}\right)$$

By substituting (15) and (16),

$$\delta_x = -\alpha_x \lambda \frac{h \sin(\theta) \cos(\gamma) - \sin(\gamma) ({}^W p_{xor} - d/2)}{h \cos(\theta)}$$

and recalling that $\tilde{x} = {}^W p_{xor} - d/2$, \tilde{x} can be explicitly expressed as

$$\tilde{x} = \frac{\cos(\theta)}{K_2} (\delta_x - K_3 \tan(\theta)) \quad (26)$$

where $K_2 = \alpha_x \lambda \frac{\sin(\gamma)}{h}$, $K_3 = -\alpha_x \lambda \cos(\gamma)$.

Equations (25) and (26) render the orientation and position errors as a function of x_v and δ_x . The design objective is to obtain a controller which, based on calculated values of errors θ and \tilde{x} , attains

$$\lim_{t \rightarrow \infty} \begin{pmatrix} \tilde{x}(t) \\ y(t) \end{pmatrix} = \begin{pmatrix} 0 \\ \int v dt + y(0) \end{pmatrix}$$

that is, the control navigation objective is asymptotically obtained. To this aim, the following control law is proposed

$$\omega_r = -K_{s\theta}(\theta) \theta - K_{s\tilde{x}}(\tilde{x}) \tilde{x} v \frac{\sin(\theta)}{\theta} \quad (27)$$

$v = \text{constant}$

where $K_{s\theta}(\theta)$ and $K_{s\tilde{x}}(\tilde{x})$ are variables designed to avoid saturation of control signals, as it will be explained later.

By considering (1) and (27) with state variables θ and \tilde{x} , the unique equilibrium point of the closed loop equation is $[0 \ 0]^T$. Asymptotic stability of the control system can be proved by regarding the following Lyapunov function

$$V(\tilde{x}, \theta) = \frac{\theta^2}{2} + \int_0^{\tilde{x}} K_{s\tilde{x}}(\eta) d\eta$$

and by applying the Krasovskii-Lasalle [10] theorem.

Saturation gains in (27) can be defined as follows [4],

$$K_{s\theta}(\theta) = \frac{K_{s1}}{a_1 + |\theta|}, \text{ where } K_{s1} > 0 \text{ and } a_1 > 0 \text{ to}$$

obtain a definite positive function. Also,

$$K_{s\tilde{x}}(\tilde{x}) = \frac{K_{s2}}{a_2 + |\tilde{x}|}, \text{ with } K_{s2} > 0, a_2 > 0.$$

The constants are selected such that the terms in (27) do not saturate the control signal ω_r . Finally, an inverse dynamics controller is regarded, like that of (21) and (22) with ω_R stated by (27).

4 FUSION OF CONTROL SIGNALS

The controllers described in Section 3 are redundant, because they have the same control objective: to guide the robot along the corridor centerline. They are based, however, in different principles, which turns difficult their fusion at sensorial level. Here, the fusion of both control commands is proposed, in order to attain a control signal that allows a robust navigation along the corridor. The fusion is made by using a Kalman filter, thus minimizing the uncertainty on calculating both control signals. This uncertainty is evaluated in terms of the sensing error and the environment conditions by introducing a time-varying covariance function for each controller [8].

A. Stability of the Control System

Let us consider that, like in Figure 6, n controllers with the same control objective are used. Then, the following set of control signals from the inverse dynamics controllers (21) are obtained,

$$\begin{aligned}\omega_{r1} &= \frac{1}{ka_\omega}(\eta_1 + b_\omega \dot{\omega} + a_\omega \omega) \\ \omega_{r2} &= \frac{1}{ka_\omega}(\eta_2 + b_\omega \dot{\omega} + a_\omega \omega) \\ &\vdots \\ \omega_{rn} &= \frac{1}{ka_\omega}(\eta_n + b_\omega \dot{\omega} + a_\omega \omega)\end{aligned}$$

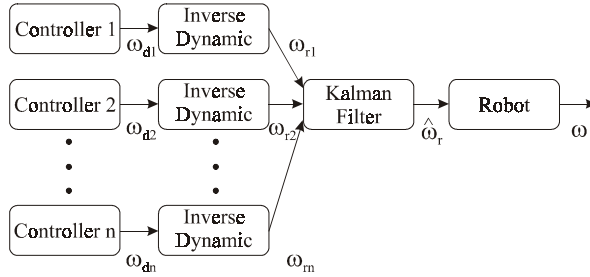


Figure 6. Output fusion of different controllers.

Then, the fused control signal is

$$\hat{\omega}_r = \frac{1}{k_\omega}(\hat{\eta} + b_\omega \dot{\omega} + a_\omega \omega) \quad (28)$$

For an ideal control command $\omega_d = \omega_{di} + \Delta\omega_{di}$ it corresponds an ideal η such that

$$\begin{aligned}\eta &= \eta_1 + \Delta\eta_1 \\ \eta &= \eta_2 + \Delta\eta_2 \\ &\vdots \\ \eta &= \eta_n + \Delta\eta_n\end{aligned}$$

or in terms of the fused signal $\hat{\eta}$,

$$\eta = \hat{\eta} + \Delta\hat{\eta} \quad (29)$$

By equating (20) and (28) and taking (29) into account

$$\hat{\eta} = \eta - \Delta\hat{\eta} = \ddot{\omega} \quad (30)$$

Now, from (22) and (30) it is possible to write the following dynamics for the angular velocity error

$$\ddot{\tilde{\omega}} + k_{d\omega} \dot{\tilde{\omega}} + k_{p\omega} \tilde{\omega} = \Delta\hat{\eta} \quad (31)$$

Defining the state vector $x = [\tilde{\omega} \quad \dot{\tilde{\omega}}]^T$, equation (31) can be written as

$$\dot{x} = Ax + \delta(x) \quad (32)$$

where

$$A = \begin{pmatrix} 0 & 1 \\ -k_{p\omega} & -k_{d\omega} \end{pmatrix} \delta(x) = \begin{pmatrix} 0 \\ \Delta\hat{\eta} \end{pmatrix}$$

Now, it can be proved that the system described by (32) has an ultimately bounded solution [10]. This means that there exist $b, c > 0$ such that for each $\alpha \in (0, c)$ there is a positive constant $T = T(\alpha)$ so that

$$\|x(t_0)\| < \alpha \Rightarrow \|x(t)\| \leq b \quad \forall t \geq t_0 + T(\alpha)$$

where b is the ultimate bound. By regarding the following Lyapunov candidate

$$V = x^T P x, \quad P = P^T > 0$$

its time derivative is

$$\dot{V} = -x^T Q x + 2x^T P \delta(x) \quad (33)$$

where $A^T P + P A = -Q$. Also, considering bounds on both terms of (33)

$$\dot{V} \leq -\lambda_{\min}(Q)\|x\|^2 + 2\lambda_{\max}(P)\|x\|\|\delta(x)\| \quad (34)$$

From (32) $\|\delta(x)\| \leq |\Delta\hat{\eta}|$. By regarding (34),

$$\dot{V} \leq -(1-\theta)\lambda_{\min}(Q)\|x\|^2 - \theta\lambda_{\min}(Q)\|x\|^2 + 2\lambda_{\max}(P)\|x\||\Delta\hat{\eta}| \quad \text{with } 0 < \theta < 1.$$

Finally, it results

$$\dot{V} \leq -(1-\theta)\lambda_{\min}(Q)\|x\|^2, \quad \forall \|x\| \geq \frac{2\lambda_{\max}(P)|\Delta\hat{\eta}|}{\lambda_{\min}(Q)\theta}$$

so that the ultimate bound be

$$b = \frac{2\lambda_{\max}(P)}{\lambda_{\min}(Q)} \sqrt{\frac{\lambda_{\max}(P)}{\lambda_{\min}(P)}} \frac{|\Delta\hat{\eta}|}{\theta}$$

Since a Kalman filter is being used to fuse the control signals, the ultimate bound on the standard deviation of ultimate error is smaller than that corresponding to the errors produced by each controller.

5 EXPERIMENTAL RESULTS

In order to evaluate the performance of the proposed control system, many experiences were done on a Pioneer 2DX mobile robot with an on-board Sony PTZ CCD camera. The images are transmitted via RF to the image processing units: one PC for optical flow calculation, and a second one for the corridor perspective lines calculation. There is a third PC to calculate the control actions and to perform their fusion. The resulting control action is sent to the robot via RF.

The optical flow calculus was realized using the Least-Mean-Square Method [6]. The corridor perspective lines are calculated using the Hough transform. The information of the image processing is updated each 200 msec . The camera constants values are: $\alpha_x = \alpha_y = 166000$ pixels/m, $\lambda = 0.0054\text{m}$, $\gamma = -5^\circ$, $h = 0.31\text{m}$. The robot navigates with linear velocity $v = 0.2\text{ m/s}$. The controllers design parameters, for the optical flow controller are set to: $k_{p\omega} = 20$, $k_{d\omega} = 1$; and for the perspective line controller to: $k_{p\omega} = 10$, $k_{d\omega} = 6$, $K_{s1} = 0.24\text{ rad/s}$, $K_{s2} = 0.48\text{ r}^2/\text{m}$, $a_1 = 0.2\text{ rad}$, $a_2 = 0.1\text{ m}$.

Figure 7 shows the trajectory of the robot navigating along a corridor at the Instituto de Automática, National University of San Juan, Argentina. The experiment is designed such that the robot finds different sensing and environment conditions during the navigation. This varying condition produces changes in the estimated variance for each controller. For the optical flow based controller, the variance represents the uncertainty of the optical flow determination. For the perspective lines based controller, the variance is proportional to the change of lines features when this change exceeds a certain bound, otherwise it is set to a minimum value. These variances evolution are shown in Figure 8. The experiment shows a good performance of the robot when navigating along the corridor centerline, independently of the varying environment conditions.

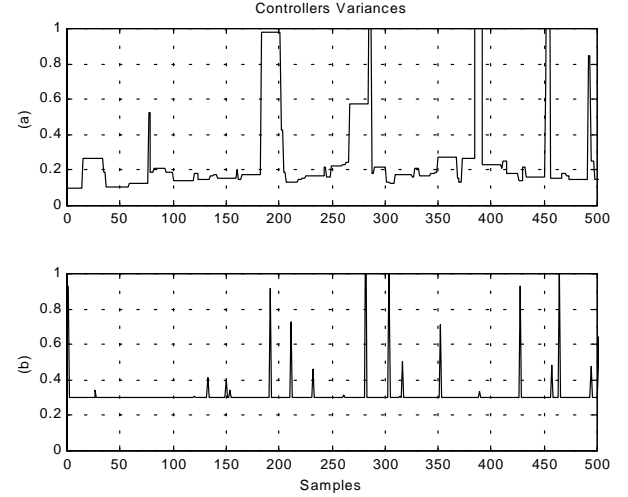


Figure 8 Time evolution of the variance of both controllers. (a) Optical flow controller variance, (b) Perspective lines controller variance.

6 CONCLUSIONS

This work has presented a control strategy for mobile robots navigating in corridors, using the fusion of control signals from vision based controllers. To this aim two controllers have been proposed: one based on the optical flow calculation and the other based on the perspective lines in the corridor. Both controllers generate angular velocity commands to keep the robot navigating along the corridor, and they compensate for the dynamics of the robot. The fusion of both control signals is made by using a Kalman filter. Stability of the resulting control system in analyzed and experiments on a laboratory robot are presented that show a good performance of the proposed controller. Future work includes the fusion of controllers based on different type of external sensors as ultrasonic and laser range sensors.

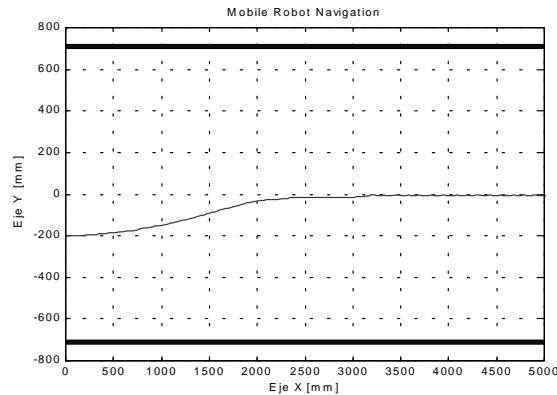


Figure 7. Trajectory of the robot in the corridor.

ACKNOWLEDGEMENTS

The authors gratefully acknowledge SETCIP and CONICET (Argentina), and CAPES (Brazil) for partially funding this research.

REFERENCES

- [1] Arkin, R. and Balch, T. AuRA: principles and practice in review. *Experimental and Theoretical Artificial Intelligence*, 9, pp. 175-189, 1997.
- [2] Barron J. , et al. Performance of optical flow techniques. *IJVC 12:1*, pp. 43-47, 1994.
- [3] Bicho, E. The dynamic approach to behavior-based robotics. *PhD. Thesis, University of Minho, Portugal*, 1999.
- [4] Carelli R. and E. Freire. Stable Corridor Navigation Controller for Sonar-Based Mobile Robots. *Technical Report, INAUT, Univ. Nac. de San Juan. Argentina*, 2001.
- [5] Dev A., et al. Navigation of a mobile robot on the temporal development of the optic flow. *Proc. Of the IEEE/RSJ/GI Int. Conf. On Intelligent Robots and Systems IROS'97, Grenoble*, pp. 558-563, 1997.
- [6] Dev A., et al. (1997). Confidence measures for image motion estimation. *RWCP Symposium, Tokio*.
- [7] Dixon W., et al. Nonlinear Control of wheeled mobile robots. *Springer Verlag*, 2001.
- [8] Freire, E. et al. Mobile robot navigation based on the fusion of control signals from different controllers. *Proceedings of the 2001 European Control Conference, pp. 1828-1833. Porto, Portugal*, 2001.
- [9] Frizera Vassallo R., et al. Visual navigation: combining visual servoing and appearance based methods. *SIRS'98, Int. Symp. on Intelligent Robotic Systems, Edinburg, Scotlnd*, 1998.
- [10] Khalil H. Non-linear systems, Second Edition. *Prentice-Hall, 1996*, 1996.
- [11] Pirjanian, P. Multiple objective behavior-based control. *Robotics and Autonomous Systems*, 31, pp. 53-60, 2000.
- [12] Rosenblatt, J. DAMN: A distributed architecture for mobile navigation". *PhD Thesis, Carnegie Melon University, USA*, 1997.
- [13] Saffiotti, A., et al. A multivaluated logic approach to integrating planning and control. *Artificial Intelligence*, 76, pp. 481-526, 1995.
- [14] Santos-Victor J., et al. Divergent stereo in autonomous navigation: from bees to robots. *Int. Journal of Computers Vision*, 14-159-177, 1995.
- [15] Servic S. and S. Ribaric. Determining the Absolute Orientation in a Corridor using Projective Geometry and Active Vision. *IEEE Trans. on Industrial Electronics*, vol. 48, No. 3, 2001.
- [16] Yang Z. and W. Tsai. Viewing corridors as right parallelepipeds for vision-based vehicle localization. *IEEE Trans. on Industrial Electronics*, vol. 46, No. 3, 1999.